Progress In Electromagnetics Research Letters, Vol. 51, 61–66, 2015

Dual-Band Bandpass Filter with Wide Upper Stopband Using Novel Stepped Impedance Stub-Loaded Quad-Mode Resonator

Lei Lin*, Zhen-Long Zhang, Shou-Jia Sun, and Chang-Hong Liang

Abstract—This paper presents a wide upper stopband dual-band bandpass filter (BPF) with controllable passband frequencies and bandwidths as well as a high out-of-band rejection level. The proposed filter is realized by utilizing a novel stepped impedance stub-loaded quad-mode resonator. All the four-mode equivalent circuits of the resonator are quarter-wavelength stepped impedance resonators (SIRs), and their fundamental resonance frequencies are used to form the passbands, so the designed filter has a compact circuit size. By controlling the impedance and length ratios of the stubs of the resonator, wide upper stopband performance is obtained. Hook-shape feed-lines and source-load coupling are applied to provide appropriate external coupling and generate three extra transmission zeros, which greatly improve the selectivity of the proposed filter. An experimental filter operating at 1.5 and 3.5 GHz is designed, fabricated, and measured for validation. The measured results have good agreement with the simulated ones.

1. INTRODUCTION

In modern wireless communication systems, multi-band microwave components are often required, and the dual-band bandpass filter (BPF) becomes a good candidate. Therefore, it is highly desirable to develop a variety of configurations to implement good performance dual-band BPFs with compact circuit size. Much research work has been done, and various design approaches have been presented. In [1–7], stub-loaded resonators (SLRs) and stepped impedance resonators (SIRs) were used to constitute dual-band BPFs. In [8], a dual-band BPF was constructed by cascading two E-type resonators. In [9], two multi-mode resonators were connected together by a grounded via to implement a 3-order dual-band BPF. All the dual-band BPFs presented above were designed using two or more resonators. For miniaturization, a variety of dual-mode resonators were proposed to design filters [10–12]. Many reports have been published about dual-mode dual-band BPFs [13–19], in which the first harmonic even- and odd-mode are utilized to form the second passband, thus leading to both passbands dependent on each other which is undesirable.

In this paper, a novel stepped impedance stub-loaded quad-mode resonator is proposed, and a dual-band BPF is designed using the four fundamental frequencies of the resonator. The fundamental frequency of each mode can be tuned freely by changing the corresponding physical dimensions and the higher harmonics can be adjusted over a wide range by changing the impedance and length ratios. So the passband center frequencies and bandwidths of the filter can be controlled independently, and a wide upper stopband can be obtained. Hook-shape feed-lines and source-load coupling are employed to generate three extra transmission zeros (TZs) to achieve good selectivity. Finally, a practical dual-band BPF operating at 1.5 and 3.5 GHz is designed, fabricated, and measured. The measured results validate the proposed design.

Received 6 December 2014, Accepted 6 January 2015, Scheduled 16 January 2015

* Corresponding author: Lei Lin (yeslinlei@gmail.com).

The authors are with the National Key Laboratory of Antennas and Microwave Technology, Xidian University, Xi'an 710071, P. R. China.

2. ANALYSIS OF THE PROPOSED QUAD-MODE RESONATOR

Figure 1 depicts the proposed stepped impedance stub-loaded quad-mode resonator, which contains four identical stepped impedance stubs at the two sides and a short-ended stub at the symmetry plane of the resonator.

Due to its symmetry, even-odd-mode method is applied to analyze the resonance characteristics of the proposed resonator. Under even-mode excitation, the symmetry plane AA' can be modeled as a magnetic wall, the short-ended stub is bisected and the width is half what it was. The even-mode equivalent circuit is shown in Figure 2(a). Under odd-mode excitation, the symmetry plane AA' behaves as an electric wall, and the short-ended stub is ignored. The odd-mode equivalent circuit is shown in Figure 2(b). It can be seen from Figure 2(a) and Figure 2(b) that the even- and odd-mode equivalent circuits are still symmetrical, and then even-odd-mode method is applied once again to analyze their operating mechanism. Figure 2(c) shows the even- and odd-mode equivalent circuits of Figure 2(a), and Figure 2(d) shows the even- and odd-mode equivalent circuits of Figure 2(b). Four modes named modes $e1$, $e2$, $o1$, and $o2$ are obtained from Figure 2(c) and Figure 2(d). Obviously, all the four-mode equivalent circuits are $\lambda/4$ SIRs, and their fundamental frequencies are named as f_{e1}, f_{e2}, f_{o1}, and f_{o2},

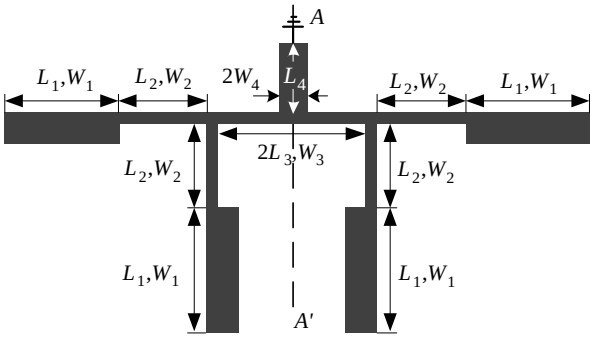

Figure 1. Schematic of the proposed stepped impedance stub-loaded quad-mode resonator.

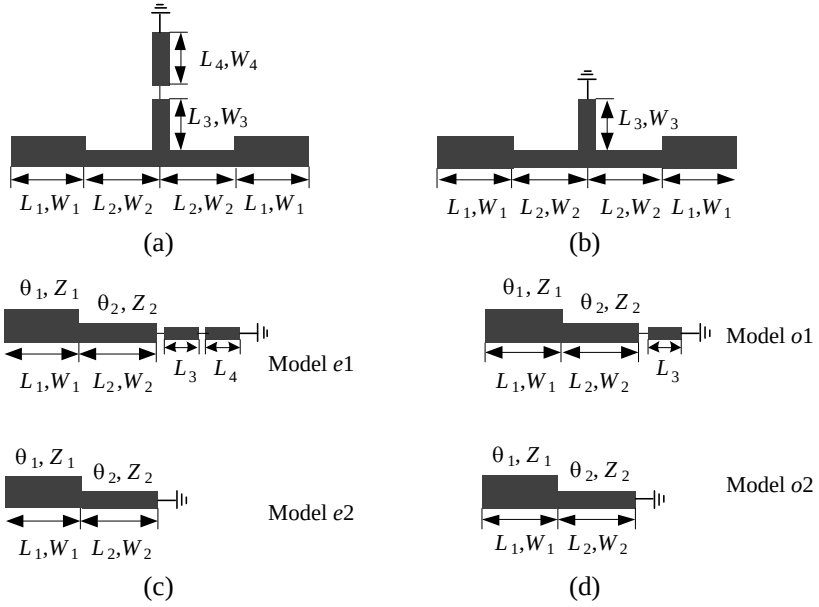

Figure 2. (a) Even-mode equivalent circuit of the quad-mode resonator. (b) Odd-mode equivalent circuit of the quad-mode resonator. (c) Even- and odd-mode equivalent circuits of Figure 2(a). (d) Even- and odd-mode equivalent circuits of Figure 2(b).

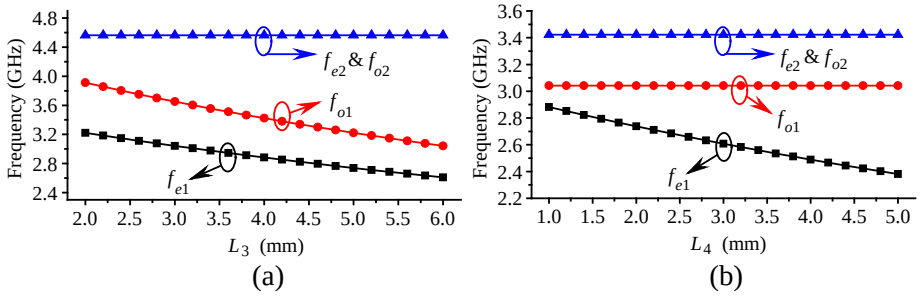

Figure 3. Resonant frequencies under different stub lengths: (a) L_3 and (b) L_4.

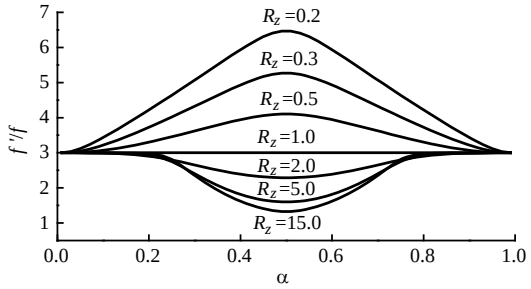

Figure 4. Frequency ratios with varied α and R_Z.

with the relationship of $f_{e1} < f_{o1} < f_{e2} = f_{o2}$.

Figure 3(a) demonstrates these four fundamental frequencies under different length L_3 (L_1 = 5.2 mm, L_2 = 6.3 mm, and L_4 = 3.0 mm), with L_3 increasing from 2.0 to 6.0 mm. It can be observed that f_{e1} decreases from 3.22 to 2.60 GHz, and f_{o1} decreases from 3.91 to 3.06 GHz, while f_{e2} and f_{o2} remain constant. Figure 3(b) illustrates these four fundamental frequencies under different length L_4 (L_1 = 6.9 mm, L_2 = 8.5 mm, and L_3 = 2.0 mm), with L_4 increasing from 1.0 to 5.0 mm, f_{e1} decreases from 2.90 to 2.39 GHz, while there is no influence on f_{o1}, f_{e2}, and f_{o2}. The same conclusions can be obtained from Figure 2(c) and Figure 2(d), it can be seen that the stub L_3 only exists in mode $e1$ and $o1$, and stub L_4 only exists in mode $e1$.

There are $\lambda/4$ SIRs in all the four modes, and their resonance conditions can be easily deduced as follows:

$$\tan(\alpha\theta_T)\tan[(1-\alpha)\theta_T] = R_Z \tag{1}$$

$$\theta_T = \theta_1 + \theta_2 \tag{2}$$

where R_Z and α are the impedance and electrical length ratios defined as:

$$R_Z = Z_1/Z_2 \tag{3}$$

$$\alpha = \theta_1/\theta_T \tag{4}$$

According to (1), the ratios of the first harmonic frequency f' to the fundamental frequency f are illustrated in Figure 4. It can be seen that the ratio f'/f can be adjusted over a wide range, which favors designing a wide upper stopband BPF using the fundamental frequencies.

3. FILTER DESIGN, FABRICATION AND MEASUREMENT

In the above section, the resonance characteristics of the proposed quad-mode resonator are theoretically analyzed. Using this, a dual-band BPF based on the quad-mode resonator was designed. In order to constitute a dual-band BPF using a single proposed quad-mode resonator, two identical resonance frequencies f_{e2} and f_{o2} have to be split to realize the passband effect. Here, two stubs were folded inward to introduce stub-stub coupling, as shown in Figure 5. It can be observed from Figure 6 that the two identical resonance frequencies f_{e2} and f_{o2} are separated.

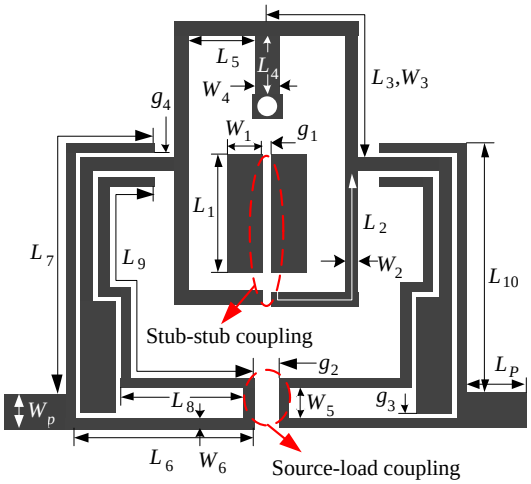

Figure 5. Layout of the proposed dual-band BPF.

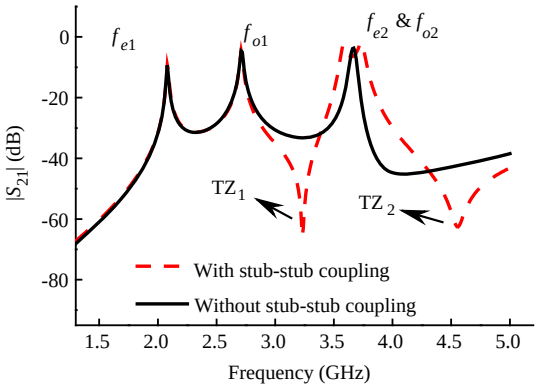

Figure 6. Simulated transmission responses with and without stub-stub coupling.

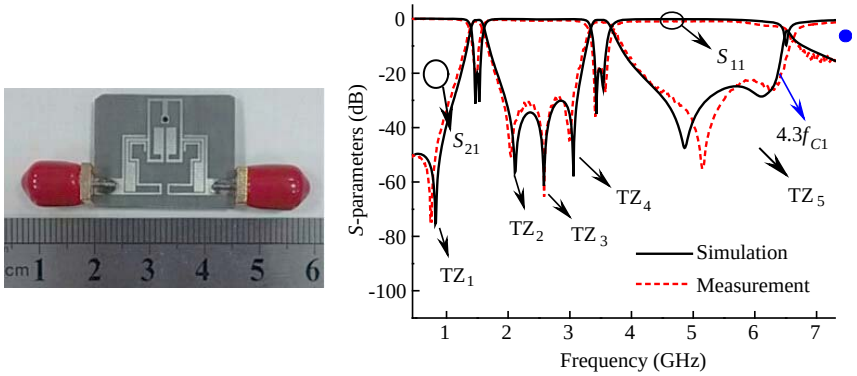

Figure 7. (a) Photograph of the fabricated dual-band BPF and (b) simulated and measured S-parameters of the proposed dual-band BPF.

The strength of stub-stub coupling can be tuned freely by the gap g_1. Two TZs are generated by stub-stub coupling and the four modes are separated into two groups, so that there are two modes in each passband, f_{e1} and f_{o1} form the lower passband, and f_{e2} and f_{o2} form the upper one.

Through the analysis, both the two passband center frequencies and in-band coupling strengths can be independently controlled by tuning the corresponding physical dimensions. The center frequency of the first passband can be tuned by L_3, and the bandwidth can be adjusted by L_4. The center frequency of the second passband can be controlled by L_1 and L_2, and the in-band coupling strength can be changed by the gap (g_1) between two folded stubs. To achieve a wide upper stopband, here, f'/f is set to be 4.5 as a design example, and the values of $\alpha = 0.43$ and $R_Z = 0.28$ are obtained from Figure 4.

As shown in Figure 5, the hook-shape feed-lines and source-load coupling are adopted to provide appropriate external coupling and achieve high selectivity. For validation, an example dual-band BPF operating at 1.5 and 3.5 GHz was designed, fabricated and measured. The simulation and optimization were carried out using Zeland IE3D software, and the dimensions are determined as follows (all in mm): $L_1 = 4.8$, $L_2 = 7.5$, $L_3 = 10.3$, $L_4 = 2.5$, $L_5 = 2.1$, $L_6 = 6.7$, $L_7 = 12$, $L_8 = 4.1$, $L_9 = 15.1$, $L_{10} = 7.7$, $L_P = 5.0$, $W_1 = 1.8$, $W_2 = 0.5$, $W_3 = 0.5$, $W_4 = 0.5$, $W_5 = 1.2$, $W_6 = 0.4$, $W_P = 2.9$, $g_1 = 0.4$, $g_2 = 1.0$, $g_3 = 0.2$, $g_4 = 0.2$.

Figure 7(a) shows the photograph of the fabricated filter, and Figure 7(b) illustrates the comparison of the simulated results and measured ones. There are five transmission zeros in Figure 7(b). The TZ$_1$

Table 1. Performance comparison between this work and filters in other papers.

Reference	Center frequencies (GHz)	$\|S_{21}\|$ (dB)	$\|S_{11}\|$ (dB)	Number of TZs	Circuit size ($\lambda_g \times \lambda_g$)
[1]	1.6/2.45	1.46/1.16	12/12	2	0.22×0.21
[8]	2.45/5.25	1.7/1.5	14/20.1	3	0.14×0.104
[14]	2.4/5.16	0.6/1.4	12 /12	4	0.46×0.42
[15]	1.51/2.4	1.11/0.4	15/16.5	5	0.14×0.09
This work	1.495/3.5	0.92/1.2	19.3/20	5	0.1×0.12

is introduced by source-load coupling, which can be controlled by the gap g_2. The TZ_2 and TZ_5 are generated by stub-stub coupling, and they can be tuned by the gap g_1. The TZ_3 and TZ_4 are produced by the hook-shape feed lines. Among them, TZ_3 is created due to the total length of hook-shape lines being $\lambda/4$ at this frequency and TZ_4 is created by the coupling between the feed lines and the resonator [20].

The measurement was performed on an Agilent 8719ES network analyzer. The measured two passband center frequencies were 1.495 and 3.5 GHz with 3 dB fractional bandwidths of 11.7% and 9.8%. The measured insertion loss was 0.96 and 1.24 dB at the center frequencies. The overall circuit size was $0.1\lambda_g \times 0.12\lambda_g$, where λ_g is the guide wavelength of the first passband. The upper stopband was extended up to 6.45 GHz ($4.3f_{C1}$) with rejection greater than 20 dB. In addition, the filter has five TZs at 0.76, 2.04, 2.58, 3.0, and 5.15 GHz with rejection of 75, 51, 65, 45 and 55 dB, respectively. Finally, Table 1 is provided to compare the proposed dual-band filter with those in [1, 8, 14, 15] in terms of a few key parameters. It is observed that the proposed filter in this paper occupies smaller size, exhibits better performance in passband and has more transmission zeros.

4. CONCLUSIONS

In this paper, a novel stepped impedance stub loaded quad-mode resonator is proposed. Each equivalent circuit of the four modes is a $\lambda/4$ SIR, so the resonator has a compact size and controllable higher harmonics. Based on the proposed resonator, a dual-band BPF (1.5/3.5 GHz) with wide upper stopband was designed. Hook-shape feed lines and source-load coupling were designed to provide appropriate external coupling and generate extra TZs. The designed filter exhibits very good in-band performance and high selectivity. Moreover, its frequencies and bandwidths can be individually adjusted. Therefore, the proposed filter will be attractive in multi-band wireless communication systems.

ACKNOWLEDGMENT

This work was supported by the National Natural Science Foundation of China (NSFC) under Project No. 61271017.

REFERENCES

1. Zhang, X. Y., C.-H. Chan, Q. Xue, and B.-J. Hu, "Dual-band bandpass filter with controllable bandwidths using two coupling paths," *IEEE Microw. Wirel. Compon. Lett.*, Vol. 20, No. 11, 616–618, Nov. 2010.
2. Kuo, J.-T. and S.-W. Lai, "New dual-band bandpass filter with wide upper rejection band," *Progress In Electromagnetics Research*, Vol. 123, 371–384, 2012.
3. Mondal, P. and M. K. Mandal, "Design of dual-band bandpass filters using stub-loaded open-loop resonators," *IEEE Trans. Microw. Theory Tech.*, Vol. 56, No. 1, 150–155, Jan. 2008.
4. Wu, G.-L., W. Mu, X.-W. Dai, and Y.-C. Jiao, "Design of novel dual-band bandpass filter with microstrip meander-loop resonator and CSRR DGS," *Progress In Electromagnetics Research*, Vol. 78, 17–24, 2008.

5. Zhang, X. Y., J.-X. Chen, Q. Xue, and S.-M. Li, "Dual-band bandpass filters using stub-loaded resonators," *IEEE Microw. Wirel. Compon. Lett.*, Vol. 17, No. 8, 583–585, Aug. 2007.
6. Kuo, J.-T., S.-C. Tang, and S.-H. Lin, "Quasi-elliptic function bandpass filter with upper stopband extension and high rejection level using cross-coupled stepped-impedance resonators," *Progress In Electromagnetics Research*, Vol. 114, 395–405, 2011.
7. Ma, D., Z.-Y. Xiao, L. Xiang, X. Wu, C. Huang, and X. Kuo, "Compact dual-band bandpass filter using folded SIR with two stubs for WLAN," *Progress In Electromagnetics Research*, Vol. 117, 357–364, 2011.
8. Zhou, M., X. Tang, and F. Xiao, "Compact dual band bandpass filter using novel E-type resonators with controllable bandwidths," *IEEE Microw. Wirel. Compon. Lett.*, Vol. 18, No. 12, 779–781, Dec. 2008.
9. Yao, Z., C. Wang, and N. Y. Kim, "A compact dual-mode dual-band bandpass filter using stepped-impedance open-loop resonators and center-loaded resonators," *Microw. Opt. Technol. Lett.*, Vol. 55, No. 12, 3000–3005, Dec. 2013.
10. Sun, S., "A dual-band bandpass filter using a single dual-mode ring resonator," *IEEE Microw. Wirel. Compon. Lett.*, Vol. 21, No. 6, 298–300, Jun. 2011.
11. Sun, S.-J., B. Wu, T. Su, K. Deng, and C.-H. Liang, "Wideband dual-mode microstrip filter using short-ended resonators with centrally loaded inductive stub," *IEEE Trans. Microw. Theory Tech.*, Vol. 60, No. 12, 3667–3673, Dec. 2012.
12. Hong, J. S. and H. Shaman, "Dual-mode microstrip open-loop resonators and filters," *IEEE Trans. Microw. Theory Tech.*, Vol. 55, No. 8, 1764–1770, Aug. 2007.
13. Fu, S., B. Wu, J. Chen, S.-J. Sun, and C. H. Liang, "Novel second-order dual-mode dual-band filters using capacitance loaded square loop resonator," *IEEE Trans. Microw. Theory Tech.*, Vol. 60, No. 3, 477–483, Mar. 2012.
14. Li, Y.-C., H. Wong, and Q. Xue, "Dual-mode dual-band bandpass filter based on a stub-loaded patch resonator," *IEEE Microw. Wirel. Compon. Lett.*, Vol. 21, No. 10, 525–527, Oct. 2011.
15. Sun, S.-J., T. Su, K. Deng, B. Wu, and C.-H. Liang, "Shorted-ended stepped-impedance dual-resonance resonator and its application to bandpass filters," *IEEE Trans. Microw. Theory Tech.*, Vol. 61, No. 9, 3209–3215, Sep. 2013.
16. Luo, S. and L. Zhu, "A novel dual-mode dual-band bandpass filter based on a single ring resonator," *IEEE Microw. Wirel. Compon. Lett.*, Vol. 19, No. 8, 497–499, Aug. 2009.
17. Sung, Y., "Dual-mode dual-band filter with band notch structures," *IEEE Microw. Wirel. Compon. Lett.*, Vol. 20, No. 2, 73–75, Feb. 2010.
18. Chiou, Y.-C., P.-S. Yang, J.-T. Kuo, and C.-Y. Wu, "Transmission zero design graph for dual-mode dual-band filter with periodic stepped-impedance ring resonator," *Progress In Electromagnetics Research*, Vol. 108, 23–36, 2010.
19. Zhao, L.-P., X.-W. Dai, Z.-X. Chen, and C.-H. Liang, "Novel design of dual-mode dual-band bandpass filter with triangular resonators," *Progress In Electromagnetics Research*, Vol. 77, 417–424, 2007.
20. Kim, C. H. and K. Chang, "Independently controllable dual-band bandpass filters using asymmetric stepped-impedance resonators," *IEEE Trans. Microw. Theory Tech.*, Vol. 59, No. 12, 3037–3047, Dec. 2011.